TSF-1005

Numerical simulation of boundary layer separation induced transition using ANSYS FLUENT user defined function

Butsangdee W, Ngiamsoongnirn K and Juntasaro E*

Mechanical and Process Engineering Department, The Sirindhorn International Thai-German Graduate School of Engineering,
King Mongkut's University of Technology North Bangkok, Bangsue, Bangkok, 10800, Thailand
*Corresponding Author: ekachaij@kmutnb.ac.th, Tel: +66 (0) 2555-2000 ext. 2926, Fax: +66 (0) 2555-2000 ext. 2922

Abstract

Laminar-to-turbulent transition plays an important role in many engineering applications. Some need turbulent flow for good mixing and transport but the others prefer laminar flow for low drag and less energy consumption. Consequently, transition prediction has become one of the major intensive research areas for decades in order to attain better understanding and be able to control the laminar-to-turbulent process. However, so far there have been only two transition models appearing in commercial CFD software: $\gamma - \mathrm{Re}_\theta$ and k_L models. Moreover, there are many factors that cause laminar-to-turbulent transition, and one of which is the separation-induced transition considered in the present paper. The objective of the current work is to present the implementation of the newly proposed transition model into the ANSYS-FLUENT software via User-Defined Function (UDF). The proposed transition model implemented here is evaluated in case of the boundary layer flow over a flat plate with a semi-circular leading edge. The simulation results are validated with the experimental data and compared against the $\gamma - \mathrm{Re}_\theta$ and k_L models in which the k_L model a baseline for the newly proposed transition model.

***Keywords**:* Separation-induced transition; Laminar kinetic energy; Intermittency; Semi-circular leading edge; Zero-pressure gradient; Boundary layer.

1. Introduction

Transition is a physical process of changing laminar flow to turbulent flow. In the past few decades, there are many researchers making an effort to study and conceive a mechanism of transition process that has been categorized as natural, bypass and separation-induced transition. [1]

Natural transition starts when the freestream turbulence level is less than 1%. Beyond a critical Reynolds number, a laminar boundary layer becomes linearly unstable and Tollmien-Schlichting waves start to grow. Since destabilizing the waves by viscosity is a subtle mechanism, the waves grow slowly and it takes farther 20 times of the distance from the leading edge to the start of linear instability to reach fully developed turbulent flow.

In case of freestream turbulence level higher than 1%, the natural transition process is bypassed such that turbulent spots are directly produced within the boundary layer by the influence of freestream disturbances. Furthermore, roughness also can cause the bypass transition due to perturbation at the wall. Moreover, bypass transition can occur when turbulent flow is injected directly into the boundary layer, e.g. cooling holes on a hot turbine blade or stator [1].

Nevertheless, it is possible that a boundary layer separation can occur while still being laminar, forming a bubble and generating turbulence in the shear layer around it and at reattachment, which penetrates into the bubble and incoming laminar flow. This kind of separation-induced transition is often associated with adverse pressure gradient and occurs, e.g., at the leading edge of an airfoil or gas turbine blades [1].

Nowadays, study of transition is widespread because transition plays an important role in (1) flow over wind-turbine blades where an optimum blade design can lead to a more efficient renewable energy system [2,3] and (2) flow over a riblet surface where the friction drag can be significantly reduced [4,5] and the manufacturing process for this kind of surface is practically possible for modern vehicle skin. [6]

From the literature review, the mathematical model has been proposed to predict transition mechanism such as transition onset and transition length. However, this paper refers two numerical models that are $\gamma - \mathrm{Re}_\theta$ by Menter [1] and k_L by Walters [8] as well as a newly proposed model, i.e., γ transport equation. The concept of $\gamma - \mathrm{Re}_\theta$ model is based on empirical transition correlations and consists of two transport equations: the intermittency equation (γ) for triggering transition locally and the second equation is solved for the transition onset momentum thickness Reynolds number (Re_θ). The k_L model has implemented an additional of transport equation (laminar kinetic energy or k_L) in order to include the effect of transitional flow. An advantage of $\gamma - \mathrm{Re}_\theta$ model is the ability to predict the transition process accurately but it is not proper to a wide range of applications because it is based on empirical correlations, in contrast to the k_L model which is based on physics. Consequently, the newly proposed model [9] combines the merit part of both transition models.

The objective of the paper is to implement the newly proposed transition model into the ANSYS-FLUENT software via User-Defined Function (UDF). The proposed transition model implemented here is evaluated in case of the boundary layer flow over a flat plate with a semi-circular leading edge to predict separation-induced transition.

2. Transition Model

2.1 The k_L transition model by Walters and Cokljat (2008)

This model can be called the three-equation transition model and can be summarized as follows:

$$\frac{\partial}{\partial x_j}\left(\rho \mu_j k\right) - \frac{\partial}{\partial x_j}\left[\left(\mu + \frac{\alpha_t}{\sigma_k}\right)\frac{\partial k}{\partial x_j}\right] = \rho P_k + \rho(R_{BP} + R_{NAT}) - \rho\omega k - \rho D_T \tag{1}$$

$$\frac{\partial}{\partial x_j}\left(\rho \mu_j k_L\right) - \frac{\partial}{\partial x_j}\left(\mu \frac{\partial k_L}{\partial x_j}\right) = \rho P_{k_L} - \rho(R_{BP} + R_{NAT}) - \rho D_T \tag{2}$$

$$\frac{\partial}{\partial x_j}(\rho u_j \omega) - \frac{\partial}{\partial x_j}\left[\left(\mu + \frac{\alpha_T}{\sigma_\omega}\right)\frac{\partial \omega}{\partial x_j}\right]$$
$$= \rho C_{\omega 1}\frac{\omega}{k}P_k + \rho\left(\frac{C_{\omega R}}{f_w} - 1\right)\frac{\omega}{k}\left(R_{BP} + R_{NAT}\right) \quad (3)$$
$$-C_{\omega 2}\omega^2 f_W{}^2 + \rho C_{\omega 3} f_\omega \alpha_T f_W{}^2 \frac{\sqrt{k}}{d^3}$$

The detail of this model can be found in Walters and Cokljat (2008) [8].

2.2 The $\gamma - \mathrm{Re}_\theta$ transition model by Langtry and Menter (2009)

This model uses an intermittency factor to control the growth rate of turbulent kinetic energy through the production and destruction terms in the turbulent kinetic energy equation in of the SST k-ω model. The turbulent kinetic energy equation controlled by the intermittency factor can be written as follows:

$$\frac{\partial}{\partial x_j}(\rho \mu_j k) - \frac{\partial}{\partial x_j}\left[(\mu + \sigma_k \mu_t)\frac{\partial k}{\partial x_j}\right] \quad (4)$$
$$= \rho \tilde{P}_k - \rho \tilde{D}_k$$

where

$$\tilde{P}_k = \gamma P_k \quad (5)$$

$$\tilde{D}_k = \min(\max(\gamma, 0.1), 1.0) D_k \quad (6)$$

The intermittency factor γ is obtained from the following modeled transport equation:

$$\frac{\partial}{\partial x_j}(\rho u_j \gamma) - \frac{\partial}{\partial x_j}\left[\left(\mu + \frac{\mu_t}{\sigma_f}\right)\frac{\partial \gamma}{\partial x_j}\right] = P_\gamma - E_\gamma \quad (7)$$

where

$$P_\gamma = F_{length} c_{a1} \rho S \left[\gamma F_{onset}\right]^{0.5}\left(1 - c_{e1}\gamma\right) \quad (8)$$

$$E_\gamma = c_{a2} \rho \Omega F_{turb} (c_{e2}\gamma - 1) \quad (9)$$

The initiation of transition is triggered by the parameter F_{onset}, while the length of transition is controlled by the parameter F_{length}. Both parameters are functions of a local transition onset momentum-thickness Reynolds number, $\tilde{R}e_{\theta t}$, that is obtained from the following modeled transport equation:

$$\frac{\partial}{\partial x_j}\left(\rho u_j \tilde{R}e_{\theta t}\right) - \frac{\partial}{\partial x_j}\left(\sigma_{\theta t}(\mu + \mu_t)\frac{\partial \tilde{R}e_{\theta t}}{\partial x_j}\right) = P_{\theta t} \quad (10)$$

where

$$P_{\theta t} = c_{\theta t}\frac{(\rho U)^2}{500\mu}\left(\mathrm{Re}_{\theta t} - \tilde{\mathrm{R}}\mathrm{e}_{\theta t}\right)\left(1.0 - F_{\theta t}\right) \quad (11)$$

However, the actual transition onset momentum-thickness Reynolds number, $Re_{\theta t}$, is obtained from the empirical correlation [1].

2.3 Newly proposed transition model

The detailed derivation of the newly proposed transition model was presented in [9]. The resulting transport equation for the intermittency factor (γ) is shown here in Eq. (13) and the computed intermittency factor (γ) is then used to control the production and destruction terms in the turbulent kinetic energy equation in Eq. (12) according to the Mentor's transition modeling concept [1],[2].

$$\frac{\partial}{\partial x_j}\left(\rho u_j k\right)-\frac{\partial}{\partial x_j}\left[\left(\nu+\sigma_k \nu_T\right)\frac{\partial k}{\partial x_j}\right] \\ =\gamma P_k-\max(\gamma,0.1)D_k \tag{12}$$

$$\frac{\partial}{\partial x_j}\left(\rho u_j \gamma\right)-\frac{\partial}{\partial x_j}\left[\left(\nu+\sigma_k \nu_T\right)\frac{\partial \gamma}{\partial x_j}\right] \\ =\frac{\gamma\left(1-\gamma\right)}{k}\cdot f_{SS}\nu_T S^2 \\ +\frac{\gamma\left(1-\gamma\right)}{k}\cdot\left(\nu+\sigma_k \nu_T\right)\cdot\frac{\partial^2 k}{\partial {x_j}^2} \\ +\frac{\gamma\left(1-\gamma\right)}{k_L}\cdot\nu\left(\frac{\partial\sqrt{k_L}}{\partial x_j}\right)^2 \\ +\frac{\gamma\left(1-\gamma\right)}{k_L}\cdot\frac{\partial}{\partial x_j}\left[\sigma_k \nu_T\frac{\partial k_L}{\partial x_j}\right] \\ +\frac{\gamma\left(1-\gamma\right)}{k_L}\left(R_{BP}+R_{NAT}\right)-\frac{\gamma^2}{k}\cdot\nu_{T,l}S^2 \\ -\gamma\left(1-\gamma\right)\cdot\beta^*\omega \tag{13}$$

In addition, the k_L equation in Eq. (2) is adopted here in cooperation with the γ equation.

3. Methodology

ANSYS-FLUENT version 14.0 software is applied to calculate and compare the novel model with the k_L model and the $\gamma-\mathrm{Re}_\theta$ model because both models exist in the ANSYS-FLUENT software. The new model is plugged into the software by transforming the written C++ code to be UDF (User defined function) code in order to be compatible with the software. However, based on the order-of-magnitude analysis, the second and fourth terms on the right-hand side of Eq. (13) are omitted because their effects are negligibly small compared to the other terms.

The simulation is performed on the T3L test cases for a flat plate with a semi-circular leading edge and the grids are created by ANSYS Workbench version 14.0 as shown in Fig. 1. There are two test cases i.e. T3L3 and T3L5, that are used to validate in this simulation with the freestream air velocity (U) of 5.0 m/s and 2.5 m/s respectively, as shown in Table.1. Inlet turbulence intensity (Tu_∞) and inlet turbulence viscosity ratio (R_μ) for both cases are adjusted in order to match the decay of the freestream turbulence intensity with the experimental data as shown in Fig. 2.

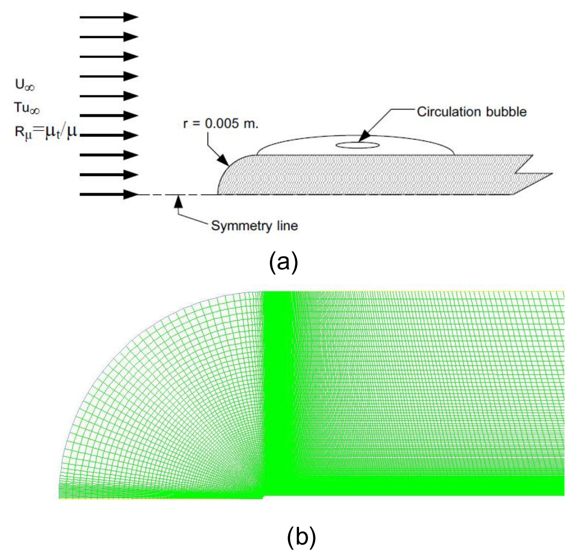

Fig. 1 (a) Geometry and (b) Mesh of T3L

Table. 1 Test cases : inlet conditions

Test case	U_∞(m/s)	Tu_∞(%)	R_μ
T3L3	5.0	2.7	13
T3L5	2.5	5.4	24

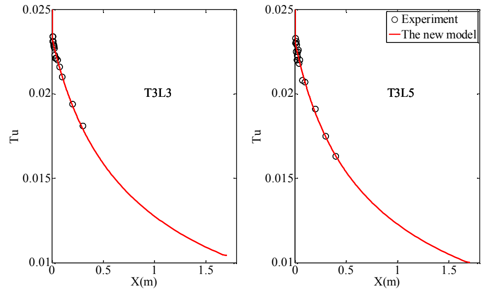

Fig. 2 The streamwise decay of freestream turbulence intensity.

Computation scheme for the simulations uses the pressure-based solver, the standard scheme for executing pressure, the second-order upwind scheme for momentum, first-order upwind for turbulence, laminar kinetic energy and specific dissipation rate. The convergence criteria is 10^{-6} for all cases.

4. Results and Discussion

The predicted skin friction coefficient (C_f) distributions for the T3L3 and T3L5 test cases are presented in the Figs. 3-4. It is found that the transition onset of both test cases is better predicted by the $\gamma - \mathrm{Re}_\theta$ model and the proposed model than the k_L model.

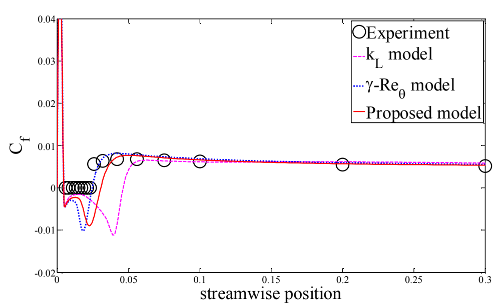

Fig. 3 Skin friction coefficient of T3L3

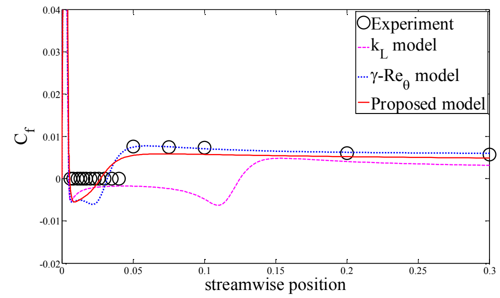

Fig. 4 Skin friction coefficient of T3L5

For T3L3 test case as shown in the Figs. 5-8, the experimental data demonstrates that the separation region in located at x=0.015 - 0.017 m and the reattachment region at x=0.021 m.

According to the velocity distribution in Figs. 5-6, it implies a boundary layer thickness. In the pre-transition region at x=0.006 m, the boundary layer is close to a wall. In the separation region, it starts at x=0.015-0.017 m where the boudary layer sets apart from the wall due to the circulation behavior deriving the adverse pressure gradient in its region. At x=0.021 m, it is the reattachment region because the boundary layer re-attachs to the wall. The last four locations at x =0.056-0.3 m indicate the velocity distributions in far downstream stations.

In Fig. 5, it is observed that all models predict the higher than the experiment. However, the proposed model can predict better than the k_L model.

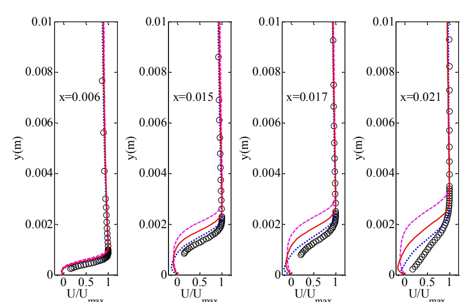

Fig. 5 Velocity distributions of T3L3 (Tu=2.7%) at

separation and reattachment regions - the legend label referring to Fig. 3

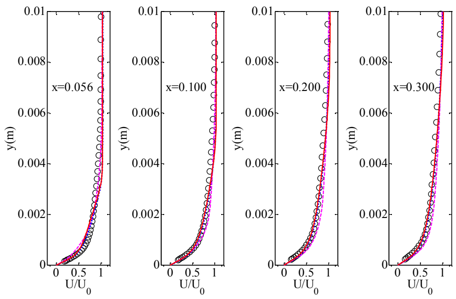

Fig. 6 Velocity distributions of T3L3 at far downstream region - the legend label referring to Fig. 3

On the other hand, the prediction of thickness is related to the prediction of u' turbulent fluctuation (u-RMS) in Fig. 7 because the underprediction of u-RMS leads to thicker spearation thickness. However, all models are capable of predicting the velocity distribution accurately in far downstream stations as shown in Fig. 6.

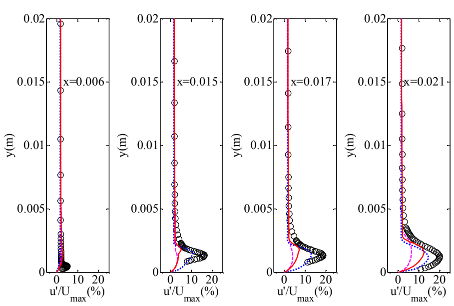

Fig. 7 u' turbulent fluctuation (u-RMS) of T3L3 - the legend label referring to Fig. 3

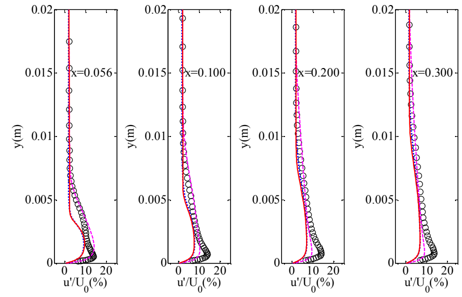

Fig. 8 u-RMS of T3L3 at far downstream region - the legend label referring to Fig. 3

The velocity profies shown in Figs. 9-10 imply that x=0.011-0.017 m is the separation region and the reattachment region at x = 0.026 m. It is significantly notice that the separation thickness predicted by the k_L model is thicker than the experiment while the others are more accurate.

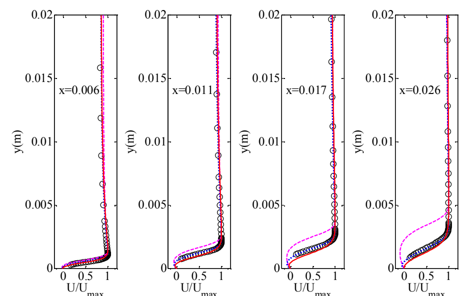

Fig. 9 Velocity distributions of T3L5 of pre-transition region at x= 0.006 m, circulation region x =0.11-0.26 m - the legend label referring to Fig. 3

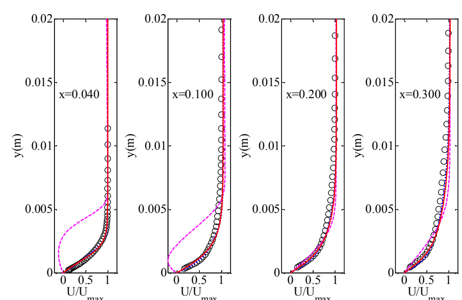

Fig. 10 Velocity distributions of T3L5 at re-attachment region - the legend label referring to Fig. 3

The predictions of u-RMS are shown in the Figs. 11-12. It is found that the under prediction of u-RMS leads to thicker separation thickness and longer reattachment. For the prediction of reattachment location by the k_L model, it is longer than the experiment - its prediction locating at x = 0.100 m while the expermental data at x = 0.026 m.

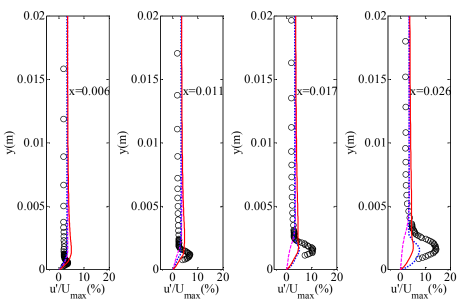

Fig. 11 u-RMS of T3L5 at pre-transition and recirculation region - the legend label referring to Fig. 3

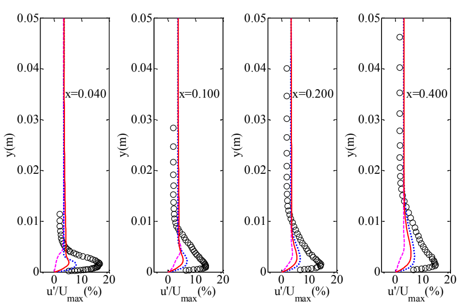

Fig. 12 u-RMS of T3L5 at reattachment region - the legend label referring to Fig. 3

Furthermore, it is noticed that the all models is better abreement with the experiment when the turbulence intensity increases e.g. the predicted separation thickness T3L5 with Tu 5.4% closer to the experimental data than T3L3 with Tu 2.7%.

5. Conclusion

The simulation results for both T3L3 and T3L5 cases demonstrate that the underprediction of u-RMS by all models leads to the overprediction of separation thickness comparing to the experimental data, particularly in the separation region. It is observed that the separation thickness prediction by the proposed model provides the simulation result closer to the experiment and better than the k_L model. However, the prediction by $\gamma - \mathrm{Re}_\theta$ model in the separation region is better than the new model. Therefore, it is required to improve of accuracy of the proposed model at in zone.

6. Acknowledgement

The authors would like to thank Assistant Professor Dr. Kyros Yakinthos for providing the T3L experimental data.

7. References

[1] Menter, R. and Langtry, B. (2009). Correlation-Based Transition Modeling for Unstructured Parallelized Computational Fluid Dynamics Codes, *AIAA Journal*, vol.47 (12), December 2009, pp. 2894-2905.

[2] Menter, F.R., Langtry, R.B., Likki, S.R., Suzen, Y.B., Huang, P.G. and Volger, S., (2004). A correlation-based transition model using local variables: Part I - Model formulation, paper presented in *the ASME Turbo Expo 2004*, *Power for Land, Sea, and Air,* June 14-17, Vienna, Austria.

[3] Piotrowski, W., Elsner, W., and Drobniak, S., (2008). Transition prediction on turbine blade profile with intermittency transport equation, paper presented in *the ASME TURBO EXPO*, June 9-13, Berlin, Germany.

[4] El-Samni, O.A., Chun, H.H., and Yoon, H.S. (2007). Drag reduction of turbulent flow over thin rectangular riblets. *International Journal of Engineering Science.* vol.45, 436-454.

[5] Peet, Y. and Sagaut, P., (2008). Turbulent drag reduction using sinusoidal riblets with triangular cross-section, paper presented in *the 38th AIAA Fluid Dynamics Conference and Exhibit*, June 23-26, Seattle, WA.

[6] Hirt, G. and Thome, M., (2008). Rolling of functional metallic surface structures. *CIRP Annuals Manufacturing Technology*. vol.57(1), 317-320.

[7] Juntasaro , E. Ngiamsoongnirn , K. and Juntasaro, V. (2012). Intermittency Algebraic Model for RANS-based Prediction of Transitional Boundary Layers on a Flat Plate with Zero Pressure Gradient, paper presented in *9th International ERCOFTAC Symposium of Engineering Turbulence Modeling and Measurements (ETMM 9)* , Thessaloniki, Greece.

[8] Walters, D. and Cokljat, D. (2009). A three-Equation Eddy-Viscosity Model for Reynolds-Averaged Navier-Stokes Simulations of Transitional, *Journal of Fluids* Engineering, vol.130 (121401), December 2008, pp. 1 – 14.

[9] Juntasaro , E., Ngiamsoongnirn , K. and Juntasaro, V. (2013). Derivation of a New γ Transport Equation for Bypass Transition, paper presented in *8th International Symposium on Turbulence and Shear Flow Phenomena (TSFP-8)* , Poitiers, France.

[10] Vlahostergios, Z., Yakinthos, K. and Goulas, A. (2009). Separation-induced boundary layer transition: Modeling with a non-linear eddy-viscosity model coupled with the laminar kinetic energy equation, *International Journal of Heat and Fluid Flow*, vol.30 , April 2009, pp. 617-636.